SCIPEDIA

Bidirectional Fluid-Structure Coupling Analysis of Steering Tool Performance with Spring Stress Consideration

Xianjun Zhou[1,*], Yuxuan Peng[1], Wenjia Cheng[2], Yangfan Xue[1] and Hao Fang[3]

[1] College of Electromechanical Engineering, China University of Petroleum (East China), Qingdao, 266580, China

[2] China Oilfield Services Limited, Tianjin, 300459, China

[3] Southwest Institute of Technical Physics, Chengdu, 610041, China

INFORMATION

Keywords:
Reservoir water injection
water distributor
flow field analysis
dynamic analysis

DOI: 10.23967/j.rimni.2025.10.60623

SCIPEDIA Revista Internacional de Métodos Numéricos para Cálculo y Diseño en Ingeniería

RIMNI Revista Internacional Métodos numéricos para cálculo y diseño en ingeniería

Bidirectional Fluid-Structure Coupling Analysis of Steering Tool Performance with Spring Stress Consideration

Xianjun Zhou[1,*], **Yuxuan Peng**[1], **Wenjia Cheng**[2], **Yangfan Xue**[1] **and Hao Fang**[3]

[1]College of Electromechanical Engineering, China University of Petroleum (East China), Qingdao, 266580, China

[2]China Oilfield Services Limited, Tianjin, 300459, China

[3]Southwest Institute of Technical Physics, Chengdu, 610041, China

ABSTRACT

This paper investigates the automatic steering tool in the integrated injection-production tubing string and proposes an analysis method for bidirectional fluid-structure coupling problems, incorporating spring stress accumulation. The pre-stress field feature in ABAQUS software is used to model the variation in leaf spring stress. A ball valve acts as an intermediary, and FLUENT software is employed to simulate the transfer of forces between the flow field and the ball valve's motion. The results indicate that the transition response time from steam injection to oil production under the designed operating conditions is approximately 0.0787 s. The motion path of the ball valve aligns with expectations, exhibiting stable movement. Additionally, an indoor simulation of the steering tool's opening and closing performance was conducted, with high-speed cameras used for experimental validation. The simulation and experimental results show a discrepancy of less than 15%, confirming the accuracy of the numerical model and providing theoretical support for the practical application of integrated injection-production tubing string technology.

OPEN ACCESS

Received: 06/11/2024

Accepted: 01/04/2025

Published: 30/06/2025

DOI
10.23967/j.rimni.2025.10.60623

Keywords:
Reservoir water injection
water distributor
flow field analysis
dynamic analysis

1 Introduction

Heavy oil, as an important part of unconventional oil and gas resources, holds an extremely important position in the world energy field [1,2]. In China, a large amount of heavy oil reserves have been discovered in basins such as Liaohe, Junggar, Songliao [3], and marine areas such as the South China Sea [4,5], and development has been carried out. The development of heavy oil resources is mainly based on the method of steam injection, using integrated injection and production technology to achieve efficient development of heavy oil thermal recovery wells. The automatic steering tool, as a key tool in the integrated injection and production column, plays an important role in the practical application of integrated injection and production technology. Based on this, a deep study of the automatic steering tool (Y-Chek) developed by RMS company was conducted, obtaining its key performance parameter curves. Through the rational use of the automatic steering tool, costs are

*Correspondence: Xianjun Zhou (zhouxianjun@upc.edu.cn).

reduced, operation efficiency is improved, and efficient development of offshore heavy oil is achieved. The steering tool has two flow channels inside and specific parts are installed inside to complete its specific functions, making the internal flow field complex. The performance analysis of the steering tool is completed based on the principle of two-way fluid-solid coupling.

Fluid-structure coupling refers to the interaction between fluid and solid, where both the fluid and solid domains must be solved simultaneously in numerical simulations. This phenomenon is characterized by strong nonlinearity and involves the exchange of energy, momentum, and mass. The research scope of fluid-structure coupling is broad, covering various fields, and the methods for analysis are typically divided into theoretical analysis and numerical simulation. Due to the complexity of two-phase media interactions, numerical methods are often employed to solve these problems. However, no single algorithm can solve all fluid-structure coupling problems, and different solution methods must be designed based on the specific characteristics of the problem at hand [6].

In China, Hu [7] deeply studied and improved the cut cell method (CCC method) based on fixed Cartesian grid and Lagrange-Euler method (ALE method), and proposed a physical simulation method suitable for swaying trees in the wind field; Wang et al. [8] took the elastic ring squeeze film damper (ERSFD) as the object, studied the deformation of the elastic ring and the pressure distribution characteristics of the internal oil film, adopted the time-sharing iterative method, and further studied the influence of vortex frequency, elastic ring thickness, number of platforms, platform width and platform height on the dynamic characteristic coefficients of the damper. Abroad, Li et al. [9] used the arbitrary Lagrange-Euler method to study the high-speed impact of water droplets with rigid planning surfaces, and compared with the two-dimensional high-speed impact experiment, proving that the adopted method and model are effective and accurate, and improved the numerical method of high-speed liquid-solid impact; Yao et al. [10] used STARCCM+ and ABAQUS to numerically study the two-way fluid-solid coupling problem of an elastic plate with one end fixed and one end free in uniform flow, and proposed a plate spacing arrangement technology to reduce the impact of wake on the vibration mode of the back plate. El Hadi Attia et al. [11] used ANSYS-Fluent for 3D CFD simulations to study the flow and heat transfer of air and TiO_2-water nanofluid. They examined the effect of TiO_2 concentration on cooling and thermal efficiency, identifying the optimal concentration. The model accuracy was validated against experimental data from the literature. Attia et al. [12] conducted CFD simulations with ANSYS to analyze the performance of a system using water and air as coolants under solar radiation (200–1000 W/m^2) and coolant flow rates (0.001–0.005 kg/s). They evaluated the impact of these factors on system performance, including temperature, thermal efficiency, and electrical output, and validated the model with experimental data from the literature. In summary, for more complex fluid-solid coupling problems, finite element simulation analysis methods are often used, but specific analysis methods often use different solution methods according to actual problems.

2 Introduction to Steering Tool Structure

The automatic steering tool (Y-Chek) is a key component for thermal recovery of heavy oil in wells, capable of integrating oil recovery and steam injection within the same well. The focus of this study is on oil wells with a casing size of 9 5/8 in. and a tubing size of 3 1/2 in. The overall structure is illustrated in Fig. 1.

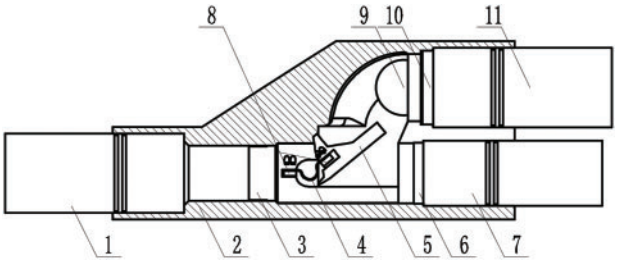

Figure 1: Internal structure diagram of automatic steering tool. 1—3 in 1/4 N.U. tubing; 2—steering tool body; 3—retaining tube; 4—irregular piece spring; 5—fork; 6—ball valve seat 1; 7—2 in 7/8 tubing; 8—stop block; 9—ball valve; 10—ball valve seat 2; 11—3 in 1/4 tubing

According to Fig. 1, the internal structure of the steering tool mainly includes a baffle tube, a special-shaped sheet spring, a stopper, a ball valve, a fork, and ball valve seats 1 and 2. The baffle tube, fork, and special-shaped sheet spring are compressed and fitted together by the stopper and bolts. Ball valve seat 2 is connected to the submersible pump as the oil recovery channel, while ball valve seat 1 is connected to the steam injection pipe as the steam injection channel. The steering tool, suspended by the submersible pump and special-shaped sheet spring, controls the position of the ball valve to switch between the oil recovery and steam injection conditions. Specifically, when the oil recovery mode is initiated, the submersible pump lifts crude oil into the steering tool, pushing the ball valve and, in turn, compressing the sheet spring until it seats on ball valve seat 1, sealing the steam injection channel. As the oil recovery increases, the formation pressure decreases, which reduces the lifting pressure of the crude oil and decreases its concentration in the produced fluid, thus lowering the output. At this point, production is halted, and steam injection begins. When the steam injection mode starts, the submersible pump is turned off. The ball valve, under the force of the sheet spring, is pushed by the fork and, due to its own gravity, seats on ball valve seat 2. Meanwhile, steam is injected from the surface into the tubing. The injected high-temperature, high-pressure steam compresses the ball valve, sealing the oil recovery channel and achieving the transition between the oil recovery and steam injection modes.

3 Steering Tool Opening and Closing Performance Analysis

For the automatic steering tool (Y-Chek) developed by RMS, a special-shaped sheet spring with a thickness of 1.2 mm and a width of 40 mm is selected. Based on the principle of fluid-solid coupling, the opening and closing performance of the integrated injection-production steering tool is studied and analyzed.

3.1 Concrete Analysis Route

Due to the complex internal flow field of the integrated injection-production automatic steering tool, and the large displacements of the fork and ball valve caused by fluid forces during their movement, multiple contacts and separations occur. Considering the design conditions of the steering tool, the entire opening and closing process is divided into the following two steps based on the complexity of the simulation analysis:

(1) Step 1 (Two-Way Fluid-Solid Coupling Problem): The ball valve, influenced by the fluid forces, moves within the bent pipe flow path inside the main body of the steering tool without making contact with the fork. This represents a conventional two-way fluid-solid coupling problem.

WORKBENCH software is employed to directly perform the two-way fluid-solid coupling simulation analysis.

(2) Step 2 (Two-Way Fluid-Solid Coupling Problem Considering Spring Stress Accumulation): After the first step, the steering tool begins to contact the fork, compressing the spring. During this phase, both the ball valve and the fork experience large displacements, with multiple contacts occurring. Due to the complexity of this interaction, it is not suitable to directly conduct two-way fluid-solid coupling simulation analysis. Therefore, based on the principles of two-way fluid-solid coupling analysis, the opening and closing performance of the steering tool is analyzed step-by-step using a weak coupling method with time-stepping iterations. The specific analysis process is outlined below.

As shown in Fig. 2, in the two-way fluid-solid coupling simulation analysis considering spring stress accumulation, the ball valve speed and fluid forces from the first-step analysis are applied as loads in the second-step simulation. Simultaneously, a displacement load is applied to the initial model of the steering tool, causing the ball valve to move to the final position of the first-step analysis. This ensures that the piece spring and fork reach the installed state, completing the preparation for the second-step simulation.

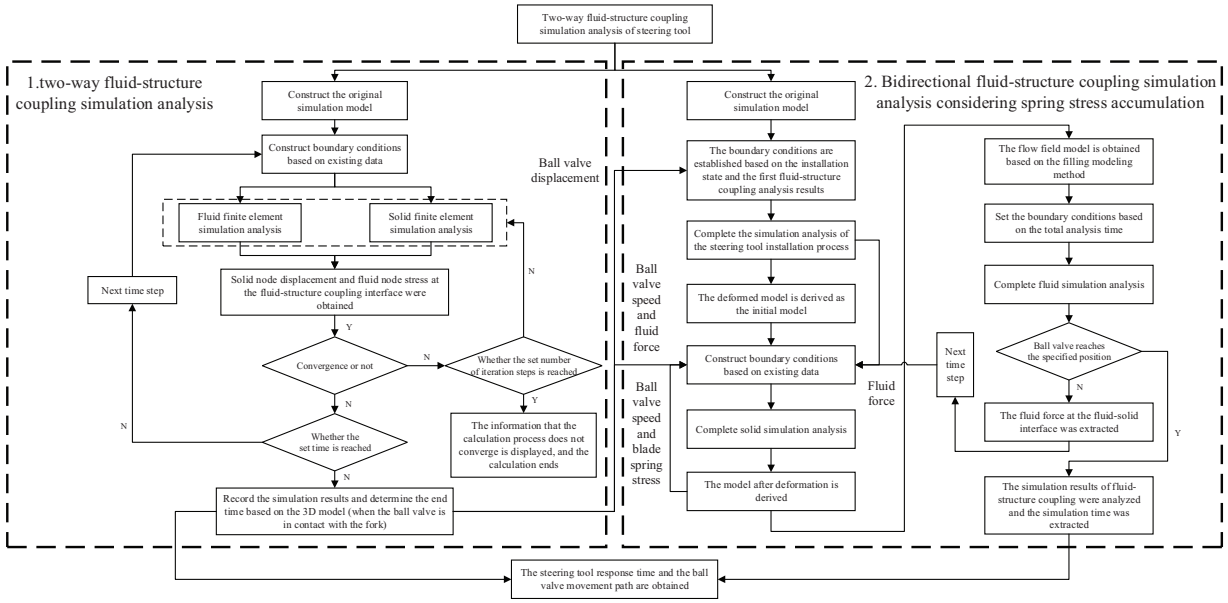

Figure 2: Steering tools performance analysis roadmap

In the second-step simulation, unlike conventional analysis methods, the solid and fluid domains are analyzed independently. The results of the previous solid analysis are incorporated into each step of the solid analysis using the predefined fields in ABAQUS software. The deformed model after loading is exported, and the fluid model is created in FLUENT software using the filling modeling method. The inlet conditions for the fluid domain are determined according to the time steps of the solid analysis, completing the fluid analysis. After several iterations, the ball valve reaches ball valve seat 1, completing the opening and closing performance analysis of the steering tool. The response time and motion path of the ball valve are then obtained. The response time can be used for real-time adjustment of ground control equipment and detection of operational status, while the motion path

of the ball valve can help verify the reliability of the steering tool, providing insights into its working process and reference for failure prevention. This analysis provides theoretical support for the practical application of integrated injection-production column technology.

3.2 Establishment of Bidirectional Fluid-Structure Coupling Model

The FLUENT and Mechanical modules in WORKBENCH are used to establish a connection, and the System Coupling environment is configured, as shown in Fig. 3, to perform the first step of the two-way fluid-solid coupling analysis [13].

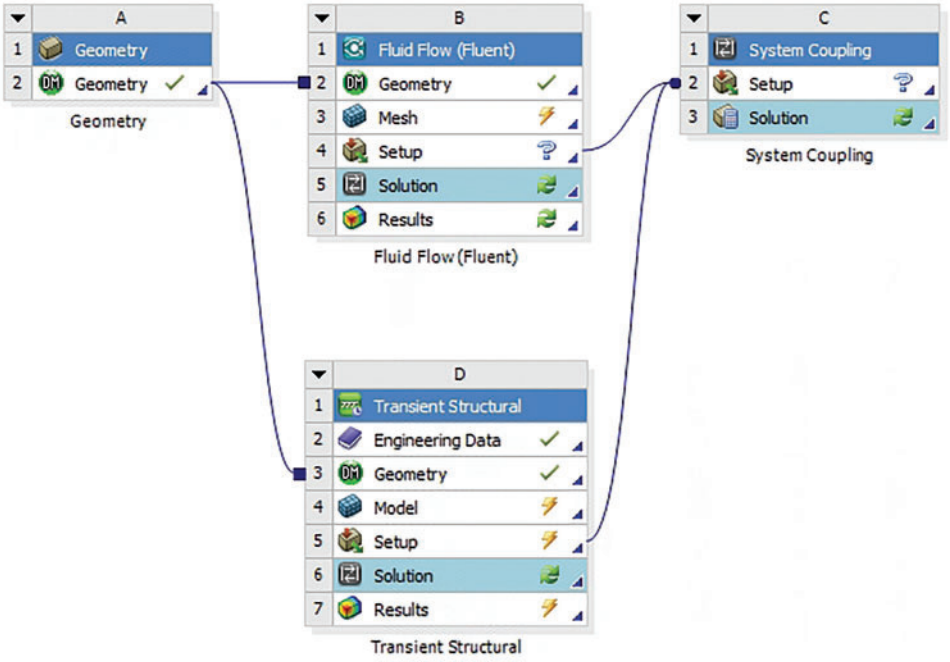

Figure 3: Two-way fluid-solid coupling module diagram

In the solid model, the fork and piece spring would create multiple small areas in the fluid model, which could reduce grid quality and cause divergence in the numerical solution. However, in the overall flow field, these components have minimal impact on the fluid flow and do not significantly affect the fluid forces at the fluid-solid interface (ball valve surface). Therefore, the piece spring and fork are excluded from the first-step simulation model of the steering tool.

As shown in Figs. 4 and 5, the fluid model is generated using the filling modeling method, based on the internal space of the solid model. In the solid model, critical parts that will interact are refined, while non-key components or those that do not participate in the analysis are assigned a grid quality above 0.1. In the fluid model, the dynamic grid areas are prioritized to ensure high grid quality, with a minimum value of 0.2 for the remaining parts. The grid division is shown in the following figure.

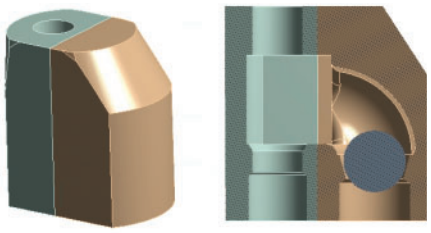

(a) (b)

Figure 4: Two-way fluid-structure coupling solid model. (a) Reduced solid model; (b) Solid model cross-section

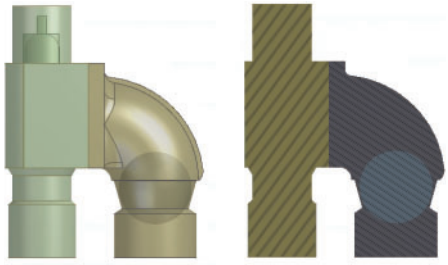

(a) (b)

Figure 5: Two-way fluid-structure coupling fluid model. (a) Fluid model; (b) Fluid model cross-section

As shown in Fig. 6, the grid in the key regions of both the solid and fluid domains is refined. In the solid domain, because the ball valve does not deform but only undergoes large displacements, there are no mass requirements for the internal grid of the ball valve, and only the surface grid quality needs to be ensured. According to the grid quality shown in Fig. 7, the minimum grid quality in the solid domain is greater than 0.13, while the minimum in the fluid domain is greater than 0.22, both of which meet the grid quality requirements for finite element analysis.

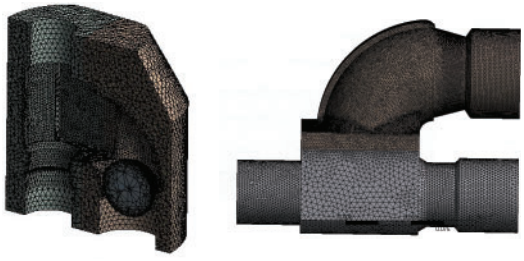

(a) (b)

Figure 6: The meshing of the two-way fluid-solid coupling model. (a) Solid grid sections; (b) Fluid meshing

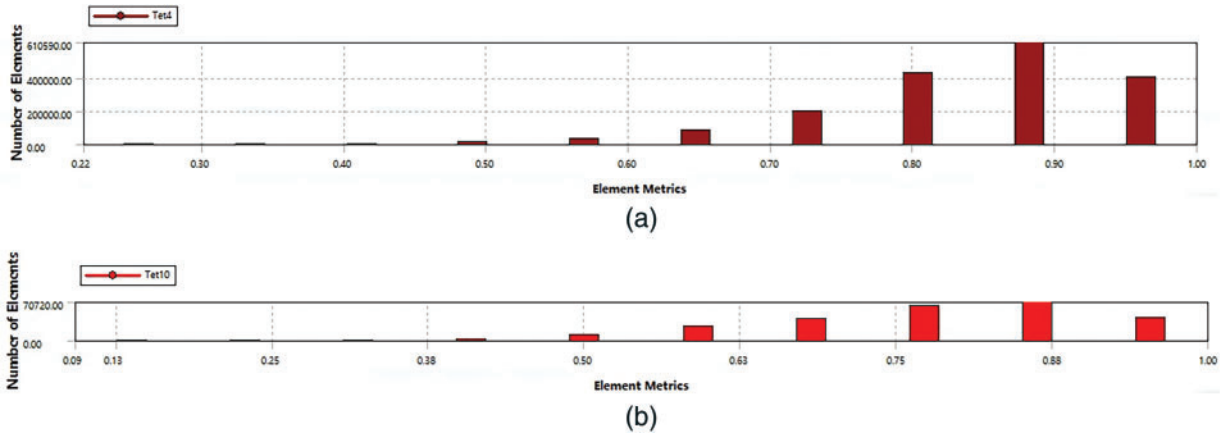

Figure 7: Mesh quality of bidirectional fluid-structure coupling model. (a) Solid mesh mass; (b) Fluid mesh mass

Based on the above model, the following assumptions are made:

1. When the submersible pump starts, the submergence (dynamic liquid level height) is neglected, and the outlet pressure is not set in the simulation.
2. Due to the good thermal insulation of the steering tool and the high-temperature, high-pressure properties of the medium, heat exchange between the tool and the environment is ignored, and temperature conditions are not set.
3. Regarding the start-up characteristics of the submersible pump: it takes approximately 0.08–0.1 s to start, and it reaches full-speed operation after 0.2 s. Based on the design conditions, the submersible pump's head must exceed 2000 m, with a flow range of 30–8000 $m^3 \cdot d^{-1}$. Given the inlet cross-sectional area, the maximum flow rate is roughly calculated to be over 40 $m \cdot s^{-1}$. Due to the rapid change in inlet flow velocity, it is assumed that the inlet flow velocity during the ball valve movement is linear with time (t), with the change trend represented as 200 t, meaning the inlet flow velocity is set as a time-dependent function.

For the first step of the steering tool simulation, the spring smoothing model and the local grid reconstruction model are employed for dynamic grid updates [14,15]. The dynamic grid areas are as follows: (1) The data exchange surface between the fluid and solid domains (the ball valve surface); (2) The region of the fluid domain where deformation occurs (the bent pipe flow channel inside the main body where the ball valve passes). Since the ball valve moves rapidly through the bent pipe flow channel in a short time, the dynamic grid control parameters are set as shown in Table 1.

The boundary and initial conditions are set as shown below, based on the actual working process of the steering tool and the operating conditions of the electric submersible pump.

To prevent the ball valve from physically contacting the flow channel wall during its movement, which could cause issues such as negative grid volumes in the fluid domain, a contact offset of 0.001 m is introduced in the solid domain, as shown in Table 2. This offset helps maintain the topological integrity of the fluid domain and improves simulation convergence.

Table 1: Dynamic mesh control parameters

Parameter type	Specific parameter
Min length scale	0.4 times the original minimum mesh size
Max length scale	1.4 times the original maximum mesh size
Max cell skewness	0.85
Max face skewness	0.85
Size remesh interval	1

Table 2: Solid domain boundary conditions and initial condition parameters

Project name	Parameter option
Bidirectional coupling computing software	ANSYS Transient Stuctural module
Object parameter	Density: 5690 $kg \cdot m^{-3}$
	Elastic modulus: 2.1×10^{11} Pa
	Poisson's ratio: 0.3
Contact condition	Contact surface: ball valve surface
	Target surface: wall of the main body inner bend flow path
	Contact type: frictionless
	Contact offset: 0.001 m
Load condition	Main body inner bend wall—fully fixed
	Ball valve face-flow field force (fluid-structure coupling data exchange)
	Solid domain—standard acceleration of gravity
Calculation time	0.2 s
Time step	0.001 s

Based on the condition parameters shown in Tables 2–4, the WORKBENCH software is employed to conduct a two-way fluid-solid coupling simulation on the bent pipe flow channel within the main body.

Table 3: Fluid domain boundary conditions and initial condition parameters

Project name	Parameter option
Bidirectional coupling computing software	ANSYS FLUENT module
Flowing medium	20.7 MPa crude oil at 250°C
Medium parameter	Density: 997.3 $kg \cdot m^{-3}$
	Dynamic viscosity: 0.004027 $Pa \cdot s^{-1}$

(Continued)

Table 3 (continued)

Project name	Parameter option
Entry boundary condition	Velocity inlet V = 200 t ($m \cdot s^{-1}$)
Exit boundary condition	Pressure outlet
Calculation time	0.2 s
Time step	0.001 s
Fluid-structure interface	The sphere cut out of the flow field

Table 4: Two-way fluid-solid coupling environment condition setting

Project name	Parameter option
Bidirectional coupling computing software	ANSYS System Coupling module
Data exchange surface	Fluid domain: interface Solid area: ball valve surface
Coupled data	Fluid domain: fluid force Solid domain: ball valve displacement (Displace)
Calculation time	0.2 s
Time step	0.001 s

3.3 Results of Bidirectional Fluid-Structure Coupling Simulation

Based on the simulation results and the steering tool assembly model in SolidWorks, it is found that when the simulation time reaches 0.0445 s, the ball valve and fork surfaces begin to make contact. Therefore, the result at 0.0445 s is selected as the final output of the first step of the two-way fluid-solid coupling analysis. With an inlet condition of 200 t, the inlet flow velocity at this time is 9.1 $m \cdot s^{-1}$. The specific analysis results are as follows.

As shown in Fig. 8, the equivalent maximum displacement of the ball valve is 88.66 mm. Fig. 9 shows that the maximum flow pressure during the ball valve's movement is 2.244×10^5 Pa. The ball valve's velocity and the fluid forces on its surface in the flow field, obtained from the previous step of the analysis, are used as initial conditions for the next step of the two-way fluid-solid coupling simulation of the steering tool. The specific data are presented in Table 5.

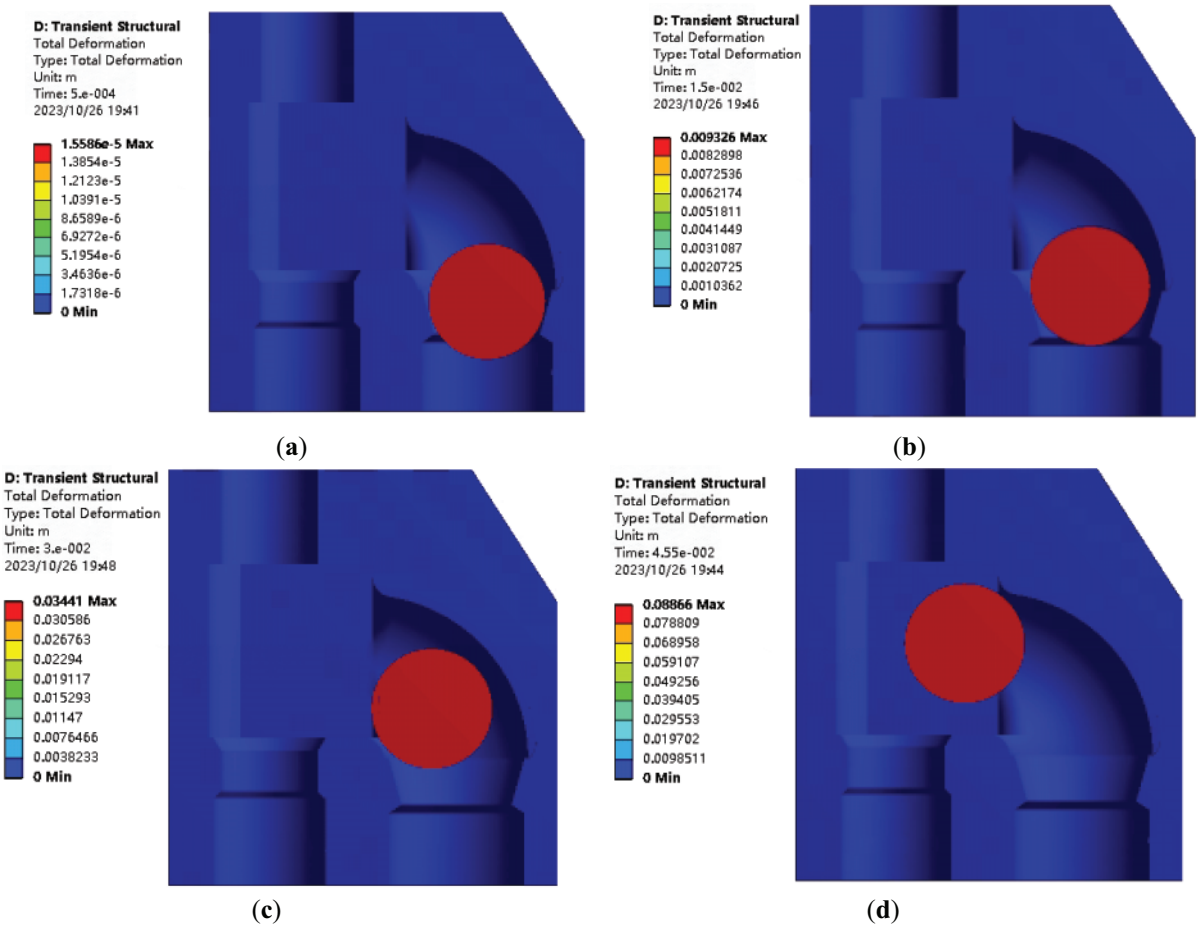

Figure 8: Total displacement cloud of solid. (a) 0.0005 s total displacement; (b) 0.015 s total displacement; (c) 0.03 s total displacement; (d) 0.0445 s total displacement

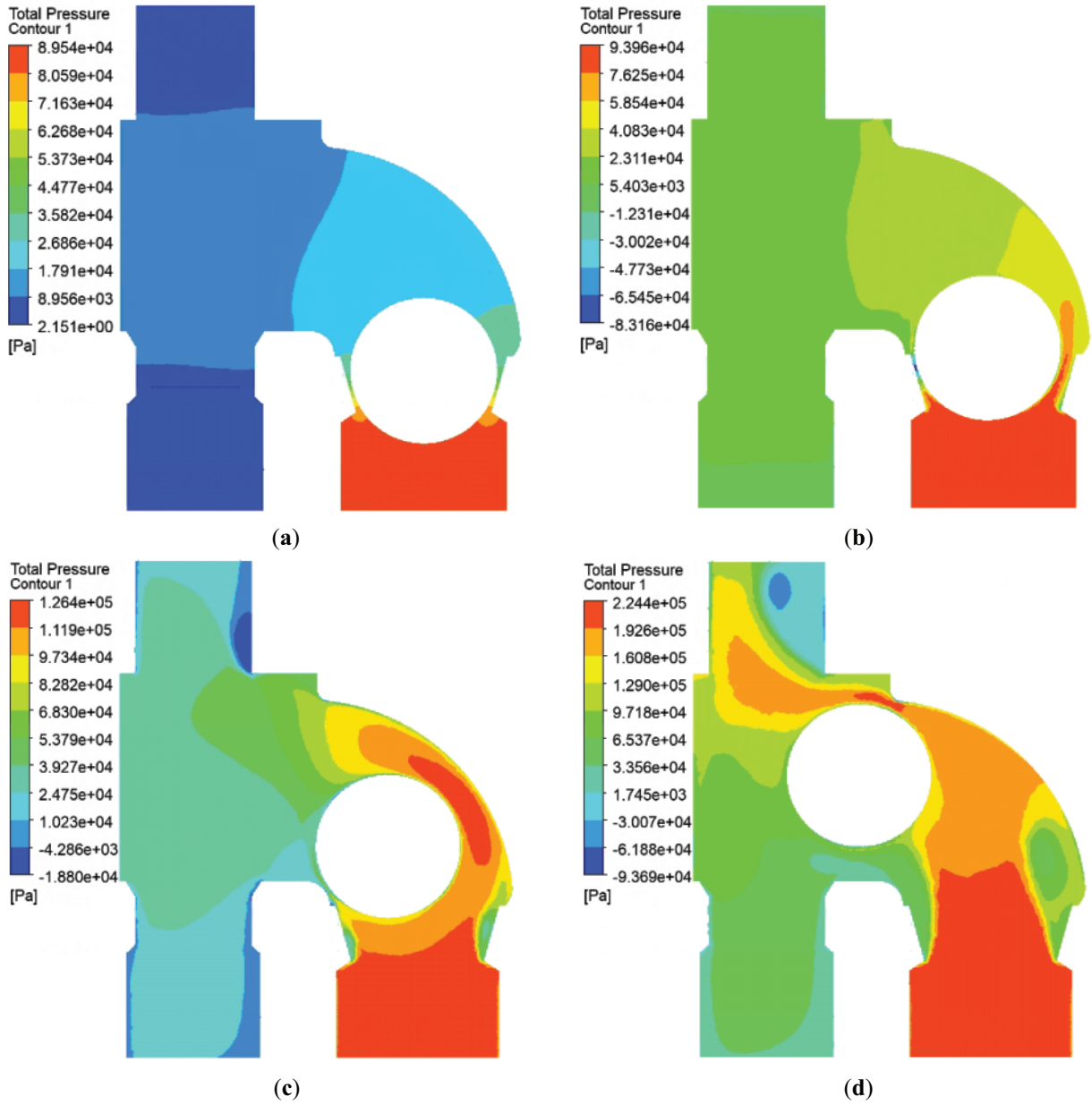

Figure 9: Total fluid pressure cloud diagram. (a) 0.0005 s total pressure; (b) 0.015 s total pressure; (c) 0.03 s total pressure; (d) 0.0445 s total pressure

Table 5: The first step two-way fluid-solid coupling simulation analysis results

Ball valve centroid speed		Ball valve mass flow force	
Average velocity on the X-axis	Y-axis average velocity	X-axial fluid force	Y-axis fluid force
$-4.067\ m{\cdot}s^{-1}$	$1.904\ m{\cdot}s^{-1}$	-19.800 N	-87.300 N

3.4 Bidirectional Fluid-Structure Coupling Simulation Analysis Considering Spring Stress Accumulation

Based on the results of the first step of the steering tool simulation analysis, the state of the internal ball valve when it reaches the contact surface of the fork, under the influence of the flow field, and the inlet flow velocity at this point are determined. Building upon this, the second step—incorporating the two-way fluid-structure interaction and the accumulation of spring stress—is carried out to complete the analysis of the steering tool's opening and closing performance.

3.4.1 The Original Installation Status is Confirmed

Because the irregular spring in the steering tool has a certain pre-tightening force when initially installed, a horizontal plate is introduced in the second step of the simulation analysis to compress the fork and achieve the installed state, thereby accounting for the actual installation condition. Since the rebound process of the spring is not analyzed, the ball valve seat 2 is excluded from this analysis. The specific model is illustrated in Fig. 10.

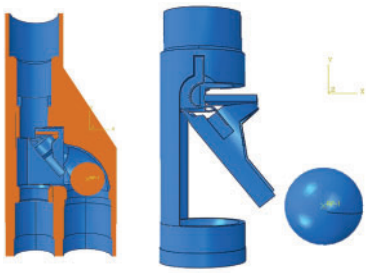

(a) **(b)**

Figure 10: Original model. (a) Model section; (b) Internal structure

According to the actual working conditions, the interior of the steering tool is filled with crude oil, which provides a certain lubricating effect. Based on the fundamental principles of friction mechanics [16], the friction coefficient between lubricated metal surfaces is approximately 0.04, and between lubricated ceramic and metal surfaces is approximately 0.1. Thus, the contact conditions for each part are established, as shown in Table 6.

As shown in Fig. 10, the key components of the entire model are comprised solely of the flat spring and ball valve. The flat spring experiences significant deformation and localized plastic deformation during the simulation analysis, thereby necessitating the adoption of the J-C constitutive model with INCONEL 718 alloy material [17].

Table 6: Steering tool spring maximum size model contact

Contact surface	Target surface	Contact type
Upper end face of the piece spring	Main body	Binding
Lower end face of the piece spring	Fork	Binding
Left side face of the fork	Main body	Friction: 0.04
Top flat face of the fork	Horizontal plate	No friction
Ball valve surface	Inner flow channel surface	Friction: 0.1
Ball valve surface	Fork	Friction: 0.1
Ball valve surface	Ball valve seat 1	No friction
Key point	Ball valve	Solid

The J-C constitutive model is influenced by temperature, flow stress, strain, and strain rate. Its specific form is expressed as follows:

$$\Sigma = (A + B\varepsilon^{n})\left(1 + C\ln\frac{\dot{\varepsilon}}{\dot{\varepsilon}_0}\right)\left(1 - \left(\frac{T - T_{room}}{T_{melt} - T_{room}}\right)^{m}\right) \tag{1}$$

In the equation: A, B, and n represent the plastic hardening parameters; C is the strain rate sensitivity coefficient; ε denotes the equivalent plastic strain; $\dot{\varepsilon}$ represents the equivalent plastic strain rate; $\dot{\varepsilon}_0$ signifies the reference strain rate, typically set at 1 s^{-1}; T stands for test temperature; T_{room} indicates the reference temperature (usually room temperature at 20°C); T_{melt} corresponds to the material's melting point temperature; and m symbolizes the temperature sensitivity coefficient.

Based on the high-temperature performance study of INCONEL 718 alloy conducted by our research group, material parameters suitable for application in the current profiled spring have been determined, as shown in Table 7 [18].

Table 7: Modified material parameters of leaf spring

Modulus of elasticity	Poisson's ratio	J-C constitutive material parameters				
		A	B	n	m	C
1.98×10^3 MPa	0.3	1205	1603	0.5164	0.9333	0.1

The sector spring, being a critical component, requires high overall grid quality due to its structural significance. The ball valve, which primarily undergoes rigid displacement, makes contact with the shift fork, the valve seat, and the internal flow channels. The ball valve itself does not exhibit stress concentration; therefore, the grid quality only needs to ensure that no penetration occurs during the simulation analysis. Based on this, the type of grid for each component and the grid division are determined. The grid quality is subsequently inspected using the 'verify mesh' command within the Mesh module. The control parameters for the grid quality check are set to the default parameters of the software. During the quality check, erroneous grids are highlighted in red, and low-quality grids are highlighted in yellow, as shown below.

As shown in Fig. 11, it can be observed that in the current model, the ball valve has not yet reached the designated position, which corresponds to its final position in the first step of the steering tool simulation analysis. Since the second step of the steering tool simulation analysis relies on the results of the first step, it is crucial to first move the ball valve to the specified position. At the same time, the sector spring and the shift fork must also be moved to their installation positions.

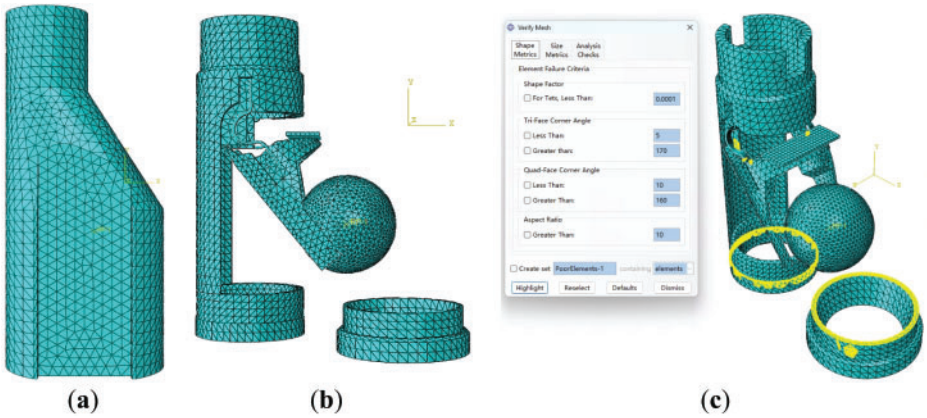

Figure 11: Steering tool spring size determination model mesh division and quality inspection. (a) Global grid; (b) Internal structure grid; (c) Internal structure grid quality detection

According to the assembly model in SolidWorks, applying a vertical displacement of -5.6 mm to the horizontal plate will compress the shift fork to achieve the installation state. Furthermore, based on the results of the first analysis, a displacement load is applied to the ball valve (key point RP-1), with displacements of -3 mm along the X-axis and -52 mm along the Y-axis, ensuring it just contacts the shift fork. This configuration establishes the initial state for the second step of the analysis, as shown in Fig. 12.

In the second step of the steering tool simulation analysis, the sector spring is continuously compressed by the ball valve, leading to an increase in internal stress as the simulation progresses. Additionally, the solid and fluid analyses are conducted independently, with each time step in the solid analysis being processed separately. As a result, the sector spring's internal stress cannot automatically inherit the results from the previous step for analysis.

To address the increasing stress in the sector spring, the predefined field feature in ABAQUS software is utilized. After establishing the predefined field for the initial solid model in the second step, the imported stress can be examined through the simulation results. Using the initial model as an example, the results of the prestress import are as follows.

As shown in Fig. 13, after the import of the prestress, the initial state of the solid simulation analysis (at time $t = 0$) exhibits a certain level of stress. The magnitude of this stress is found to be entirely consistent with the results from the previous analysis step (referring to the original installation results of the steering tool). This confirms that the imported prestress field is functioning as expected.

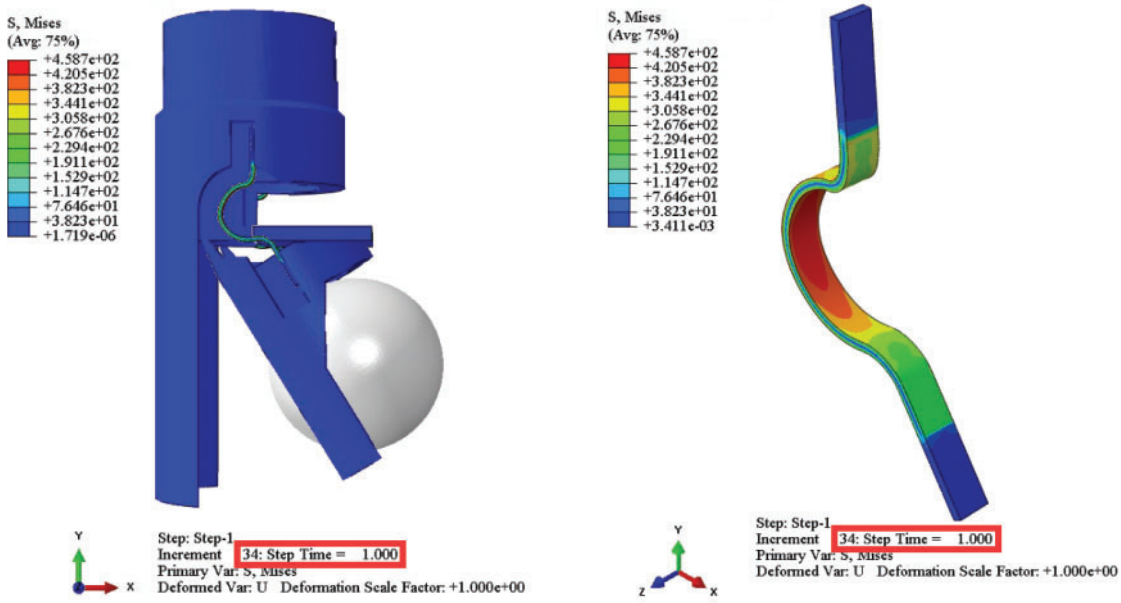

(**a**) (**b**)

Figure 12: Pivot tool initial installation status. (a) Global equivalent stress cloud map; (b) Nephogram of leaf spring equivalent stress

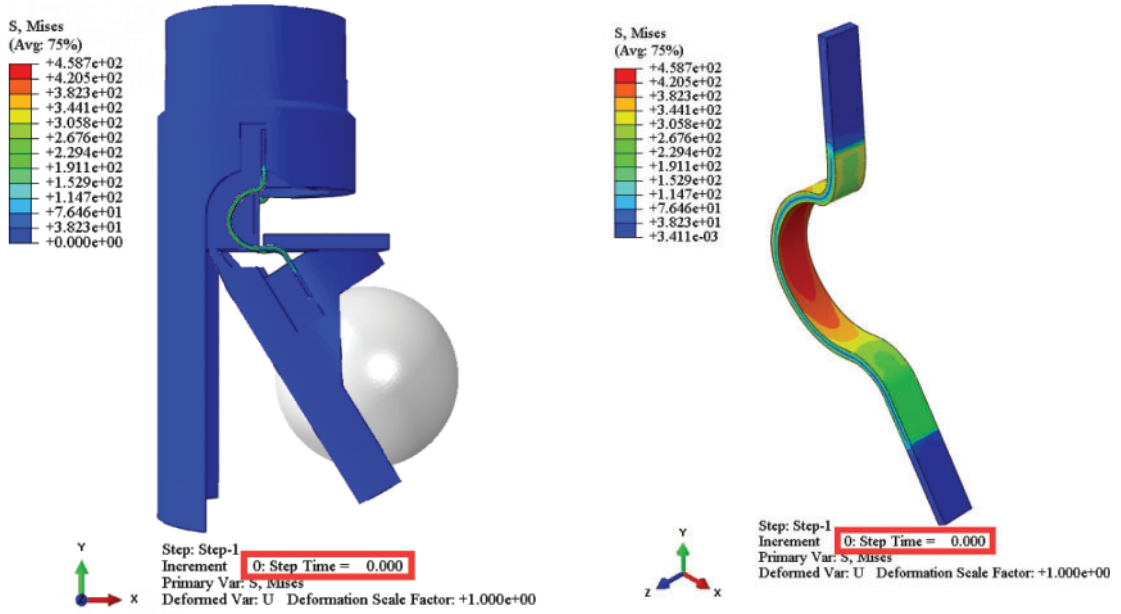

(**a**) (**b**)

Figure 13: Prestress import results. (a) Induced stress result; (b) Prestressing of blade spring

3.4.2 Simulation Analysis Result

Upon completion of the predefined field setup, the time step size is determined based on the actual simulation conditions. Taking the initial model analysis as an example, when the ball valve first comes into contact with the shift fork, the presence of the sector spring causes the shift fork to move the ball valve along the contact surface until the ball valve reaches a suitable position to begin driving the shift fork. Based on multiple simulation analyses, it has been determined that a time step of 0.01 s is reasonably appropriate. The analysis results are shown in Fig. 14.

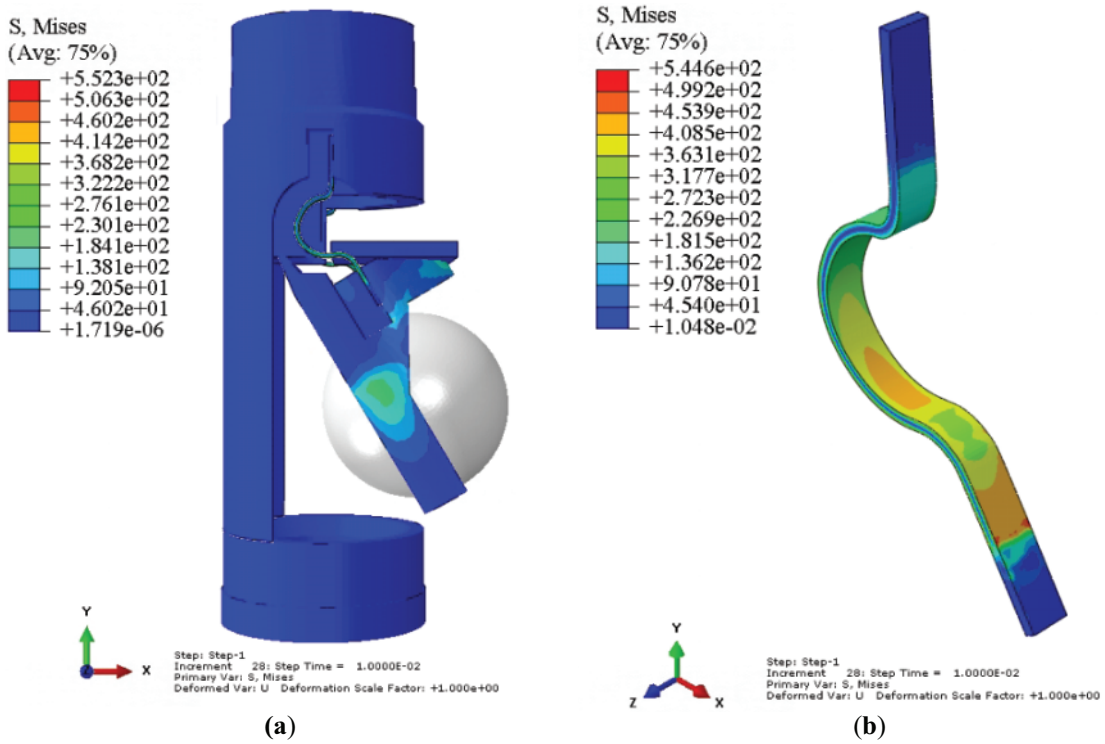

Figure 14: Results of initial solid model simulation. (a) Initial model simulation analysis results; (b) Initial deformation of blade spring

Based on the solid simulation analysis results of the initial model in the second step of bidirectional fluid-structure interaction, the ball valve velocity is extracted, with the X-axis velocity being -641.934 mm·s^{-1} and the Y-axis velocity being -1134.250 mm·s^{-1}.

As shown in Fig. 14, in the solid simulation analysis of the initial model, the ball valve undergoes only minimal movement along the contact surface of the shift fork. The impact of this movement on the flow field is minimal; therefore, the changes in the flow field forces during this process can be neglected. The study should focus on the changes in the flow field forces after the ball valve moves.

By exporting the deformation model of the sector spring and importing it into SolidWorks 3D CAD software, a steering tool assembly model is created. Subsequently, this model is imported into FLUENT software, where a flow field model is constructed using the filling modeling method, as shown in Fig. 15.

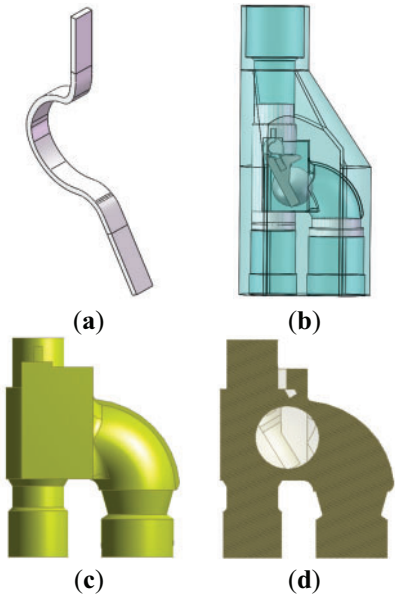

Figure 15: Step 2 two-way fluid-structure coupling fluid model. (a) Leaf spring derived model; (b) Assembly perspective model; (c) Fluid model; (d) Fluid cross-section model

As shown in Fig. 16, the fluid model grid in the second step of the steering tool simulation is relatively complex. Subsequent models must be processed according to the actual conditions to ensure high grid quality, thereby guaranteeing the accuracy of the flow field analysis.

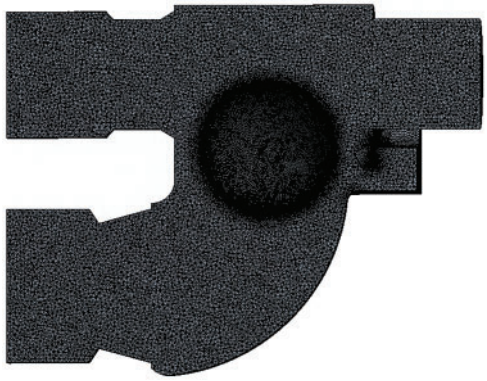

Figure 16: Fluid meshing

Given that the inlet condition is a time-varying velocity, the inlet velocity must be determined based on the total analysis time. Taking the exported model from the solid simulation analysis results of the initial model in the second step as an example, the total analysis time (the sum of the analysis time from the first step and the analysis time from the initial model in the second step of bidirectional fluid-structure interaction) is 0.0545 s (0.0445 s + 0.01 s). According to the inlet velocity model discussed earlier in the flow channel optimization, the inlet velocity at this time should be 10.9 mm·s^{-1}. The analysis results are shown in Fig. 17.

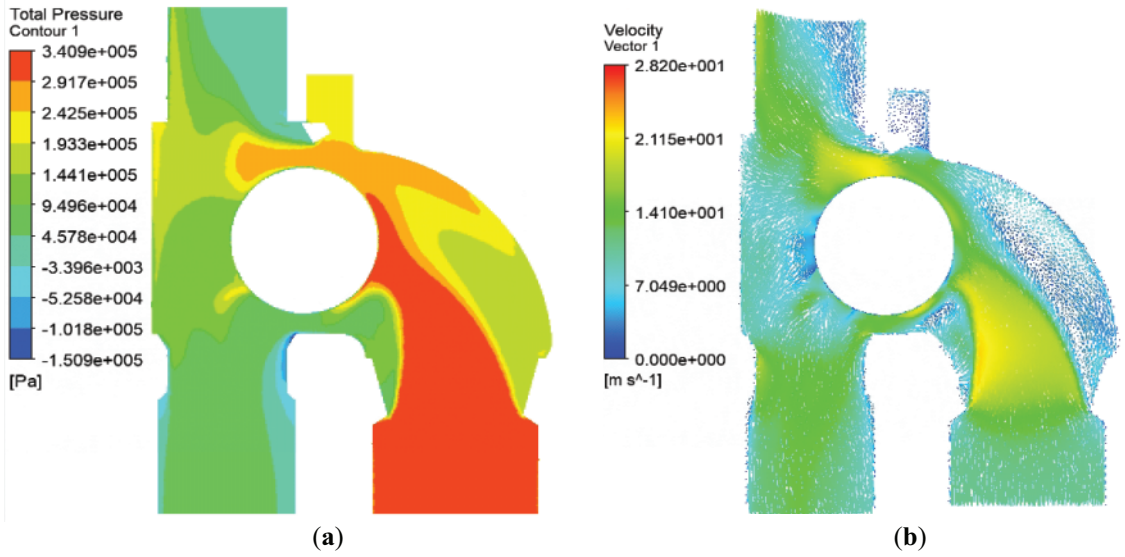

(**a**) (**b**)

Figure 17: Initial model fluid simulation results. (a) Total pressure cloud picture; (b) Velocity nephogram

Based on the fluid simulation analysis results of the initial model in the second step, the magnitude of the fluid forces on the ball valve surface is extracted, with the X-axis force being -277.480 N and the Y-axis force being -78.880 N.

By repeating the aforementioned analysis process and progressively transferring data, the bidirectional fluid-structure interaction simulation analysis for the second step of the steering tool is ultimately completed. The analysis results are shown in the figure below.

As shown in Fig. 18, the total analysis time for the second step of the steering tool is 0.0342 s. In the solid analysis, due to the uncertainty regarding the exact time at which the ball valve reaches the designated position (valve seat 1), the time step from the previous step is continued in the final analysis. The initial contact of the ball valve with valve seat 1 is then determined based on the velocity of the ball valve in the analysis results. Specifically, when the ball valve contacts valve seat 1, a rebound occurs, and the velocity of the ball valve undergoes a sudden change, with its velocity in the Y-axis direction changing from negative to positive. According to the analysis results, in the final step of the solid analysis, when the analysis time reaches 0.0042 s, a sudden change in the velocity of the ball valve is observed, indicating that the ball valve begins to contact valve seat 1 and reaches the designated position. This completes the bidirectional fluid-structure interaction simulation analysis of the steering tool, considering the accumulation of spring stress.

3.4.3 Steering Tool Performance Analysis

Based on the bidirectional fluid-structure interaction simulation analysis results from the first and second steps of the steering tool, as discussed earlier, it is determined that the time required for the steering tool to switch from the steam injection channel to the oil extraction channel is approximately 0.0787 s (0.0445 s + 0.0342 s). The displacement data of the ball valve from the simulation analysis results are extracted, and the trajectory curve of the ball valve's motion is plotted using Origin software, as shown below.

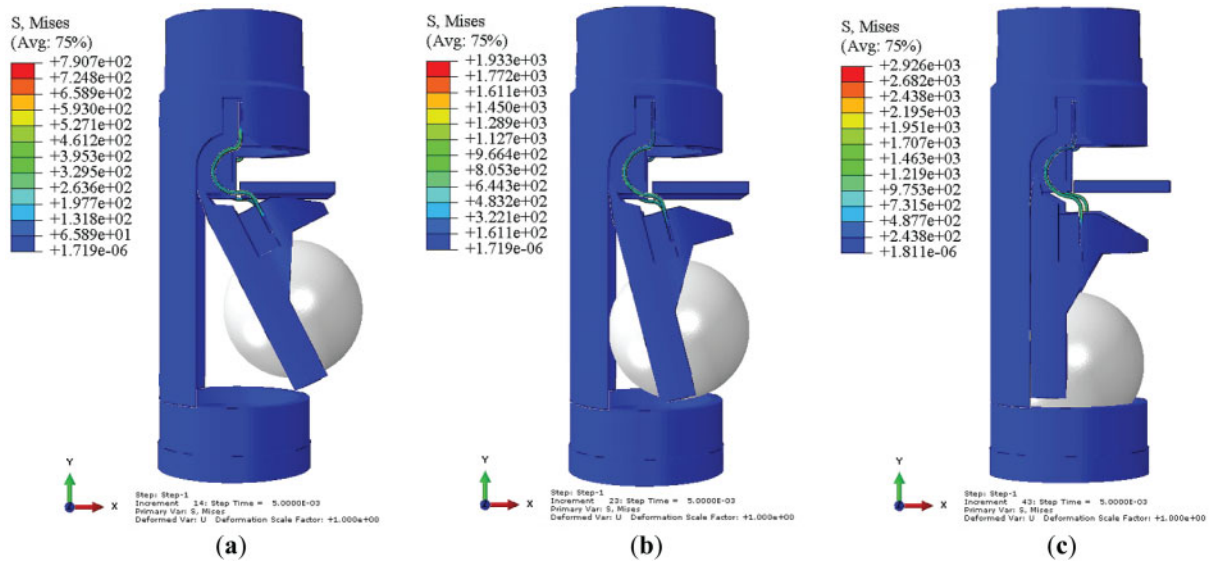

Figure 18: Solid domain partial analysis results. (a) 0.015 s; (b) 0.025 s; (c) 0.0342 s

The displacement data of the ball valve from the simulation analysis results are extracted, and the trajectory curve of the ball valve's motion is depicted using Origin software, as illustrated in Fig. 19.

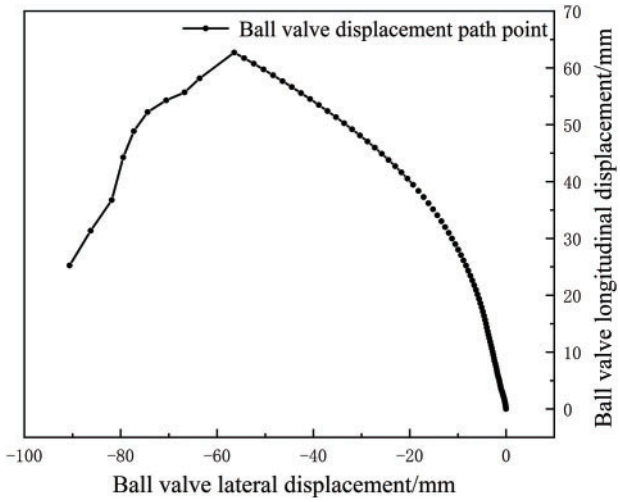

Figure 19: Ball valve movement path under steam injection to oil production condition

4 Steering Tool Opening and Closing Performance Test

To analyze and verify the actual working conditions of the integrated automatic steering tool for injection and extraction, an indoor test rig is constructed using a sector spring with a thickness of 1.2 mm and a width of 4 mm for the experiment.

4.1 Test Condition

Since the actual movement of the internal ball valve of the steering tool is directly related to the inlet fluid pump and the fluid medium, and the actual working parameters, such as the power and flow rate of the electric submersible pump, as well as the harsh conditions of crude oil, make it too costly to replicate the actual working conditions of the steering tool. Therefore, in this experiment, a conventional centrifugal pump (model 65-125-3 vertical centrifugal pump) is selected as the fluid pump, and water at normal temperature and pressure is chosen as the fluid medium for the indoor experiment. Based on this, before conducting the indoor test, the opening and closing performance simulation analysis is performed based on the test conditions using the performance analysis method discussed earlier.

4.2 Simulation Result Analysis

The simulation analysis indicates that under the test conditions, the ball valve does not reach the designed position and instead exhibits continuous compression and rebound vibrations. Therefore, the position where the ball valve first reaches its farthest point is selected as the end position, and the movement time of the ball valve is approximately 0.384 s. The motion data of the ball valve in the fluid-structure coupling of the steering tool are extracted, and its motion path is plotted using Origin software, as shown in Fig. 20.

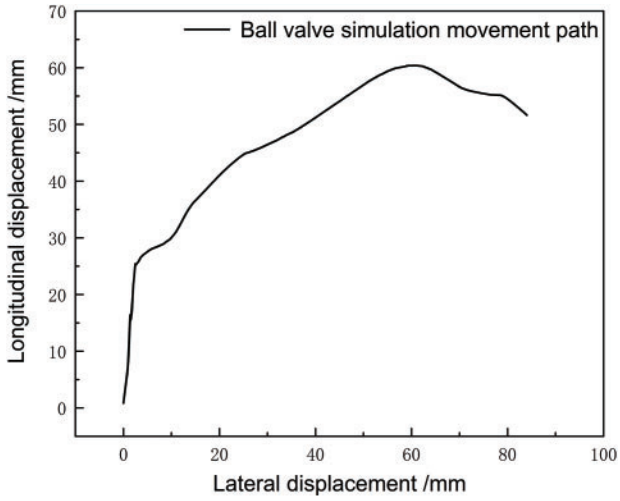

Figure 20: Indoor conditions ball valve simulation movement path

Based on the simulation analysis results under the experimental conditions of the steering tool, it is evident that the flow rate of the conventional centrifugal pump significantly differs from the actual pump flow rate, resulting in insufficient force in the flow field to push the ball valve and compress the sector spring. However, the accuracy of the simulation analysis can be verified and support provided for the analytical approach and results of this paper by comparing the motion trajectory and time of the ball valve in both the experimental and simulation results under the same conditions.

4.3 Steering Tool Laboratory Test

4.3.1 Laboratory Test Equipment

The specific test flowchart of this steering tool laboratory test is shown in Fig. 21. In the indoor experiment of the steering tool, a high-speed camera is used to capture the motion of the internal ball valve. Therefore, the overall shell of the steering tool must have sufficient strength and good light transmittance. At the same time, the color of the internal parts must be distinct from the fluid and non-transparent. After machining the ball valve and the shift fork, their surfaces are treated to a matte black finish. Based on the aforementioned experimental requirements, the shell of the steering tool, the valve seat, the blocking tube, and all the oil pipes are made from colorless and transparent acrylic material. The materials for the ball valve and the shift fork are actual materials, namely zirconia and 42CrMn alloy, respectively. The material for the sector spring is the same as mentioned in the previous section. The CCD high-speed camera used in this test and the test tooling assembled as a whole are shown in Fig. 22.

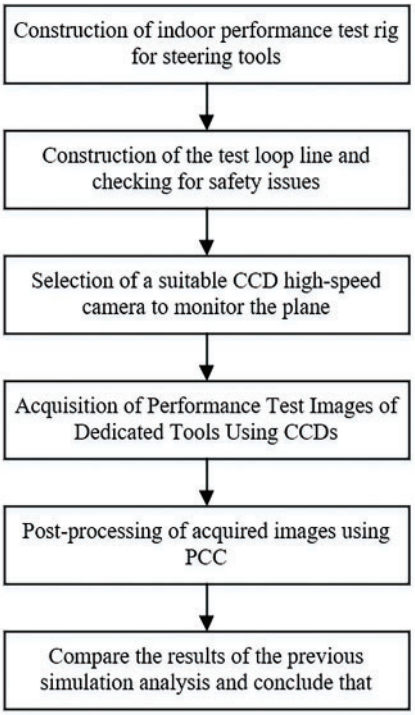

Figure 21: Laboratory test process roadmap

The main equipment used in the experiment consists of the following:

1. The experimental rig and test bench for the automatic steering tool.
2. A CCD high-speed camera used to record the motion of the internal ball valve at different moments, with the model number 310L.
3. A vertical centrifugal pump used to circulate water in the experimental pipeline at a specific flow rate, with parameters: flow rate 25 m^3/h, head 12.5 m, and model number 65-125-3.
4. A flat-panel light source used to illuminate the CCD high-speed camera.
5. A 1 m^3 horizontal water tank used to supply water for pipeline circulation.

6. A Kavite turbine flowmeter used to measure the flow rate in the pipeline.

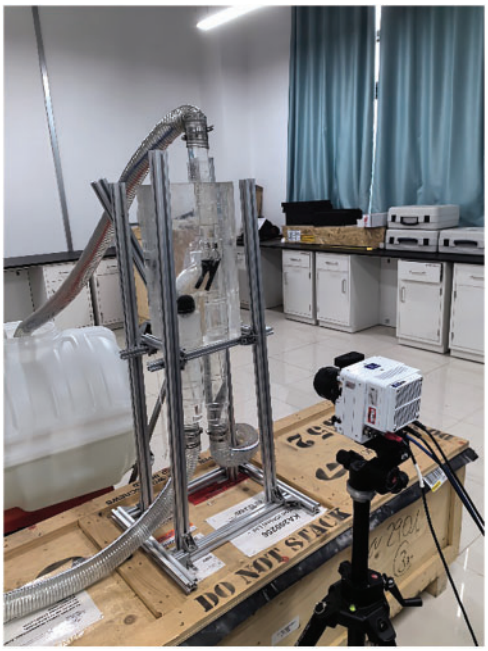

Figure 22: High-speed ccd camera

4.3.2 Specific Test Procedure

1. Experimental Loop Pipeline Setup: The experimental rig for the automatic steering tool, the pipeline centrifugal pump, flowmeter, and other recirculation pipeline equipment are connected using PVC wire-reinforced hoses. The centrifugal pump is activated to operate the recirculation pipeline, and the connections at each joint are checked to ensure they are secure, without any leakage or safety issues.
2. Determination of the Monitoring Plane: electing an appropriate monitoring plane is a critical step in the performance testing of the steering tool. Since a CCD high-speed camera is used to capture the motion of the internal ball valve, it is necessary to control the light source to ensure it illuminates the entire motion space of the ball valve when external light is directed onto the CCD camera. The camera angle and focal length are adjusted based on the imaging results to ensure the accuracy of the CCD high-speed camera's imaging, as shown in Fig. 23.

4.3.3 Image Analysis of Test Results

As shown in Fig. 24, 0.434 s after the pump starts, the ball valve inside the steering tool reaches its first farthest position, which is the designated endpoint. Based on the experimental results, the trajectory curve of the entire motion process of the ball valve is plotted using the principles of moving target detection and tracking in MATLAB software, as shown below.

According to the motion tracking results of the ball valve shown in Fig. 25, due to the similar color brightness of the ball valve and the shift fork, when the ball valve contacts the shift fork, the shift fork partially obscures the ball valve, resulting in a significant reduction in the tracking accuracy

after contact. Therefore, by extracting the motion points and using Origin software to correct and plot the ball valve's motion trajectory, the results are shown in Fig. 26.

Figure 23: CCD high-speed camera captures the target surface

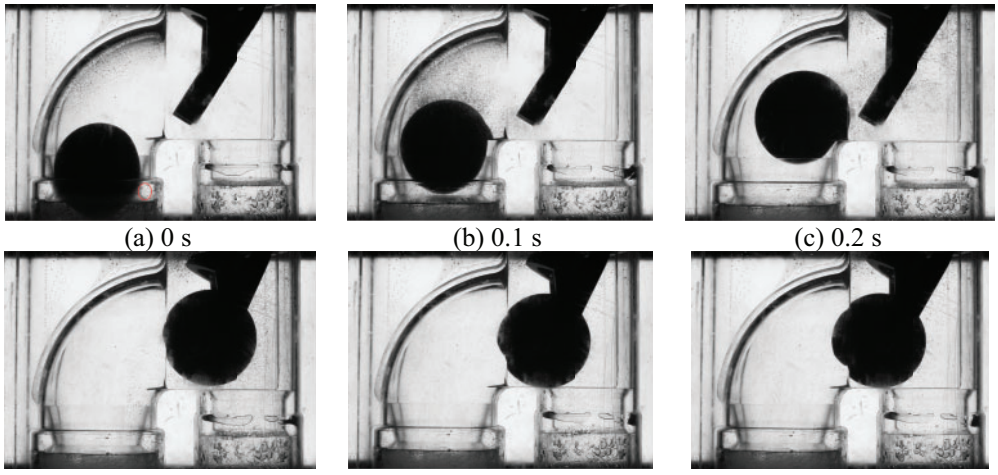

Figure 24: Steering tool test results diagram

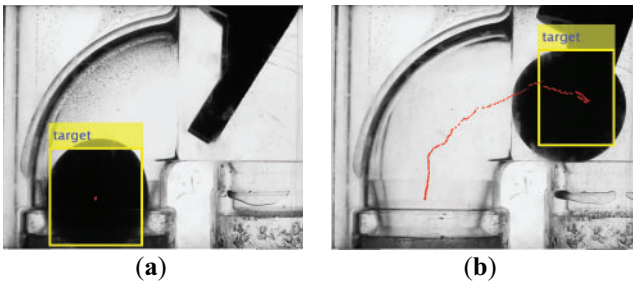

Figure 25: Ball valve motion tracking results. (a) Motion initiation; (b) Final point of motion

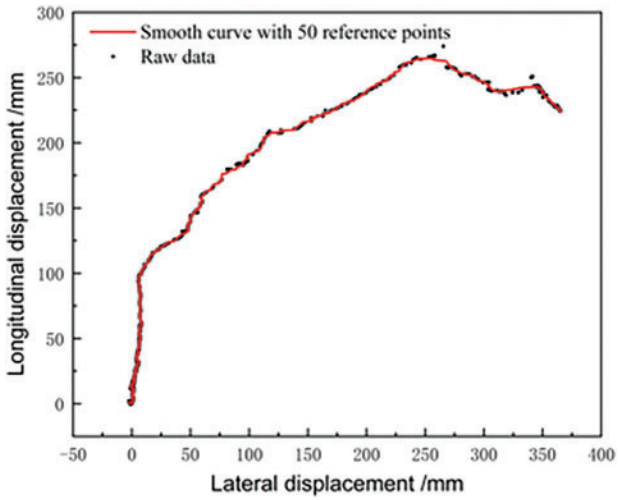

Figure 26: Ball valve path

4.4 Comparison of Simulation and Test Results

Based on the actual working conditions of the steering tool and the simulation analysis results under experimental conditions discussed earlier, the simulated motion time is approximately 0.384 s, while the actual motion time of the ball valve is 0.434 s, resulting in an error of approximately −11.5%. Additionally, as shown in Figs. 20 and 26, the overall trend of the actual and simulated motion trajectories of the ball valve is essentially consistent. However, since the actual motion trajectory of the ball valve is tracked and plotted based on the captured pixel points using MATLAB, the displacement is not the true displacement. By scaling the ball valve displacement according to the actual model size, a scaling factor of 0.23 is derived. The actual displacement curve is obtained and compared with the simulation results, as shown in Fig. 27.

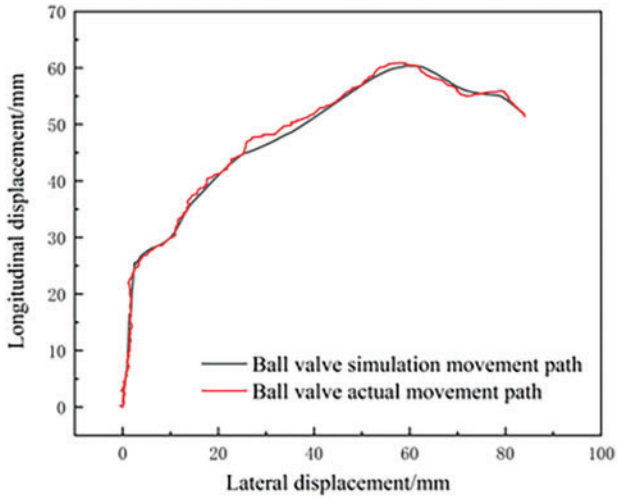

Figure 27: Ball valve motion path comparison diagram

Based on Fig. 28, it can be observed that under indoor conditions, the error range between the actual and simulated motion trajectories of the ball valve in the steering tool is within ±15%. The initial start-up phase exhibits a larger discrepancy between the experiment and simulation, primarily due to the very short buffering time when the fluid pump starts, while the simulation analysis assumes a stable flow velocity. This leads to a significant motion error at the initial position. However, after the flow field stabilizes, the motion path of the ball valve closely matches. Based on the experimental and simulation results of the steering tool, the accuracy of the finite element simulation analysis and the effectiveness of the performance analysis method for the steering tool are validated. These analyses can effectively evaluate and predict the motion of the ball valve within the steering tool, providing valuable insights for its practical application in integrated injection and extraction pipe columns.

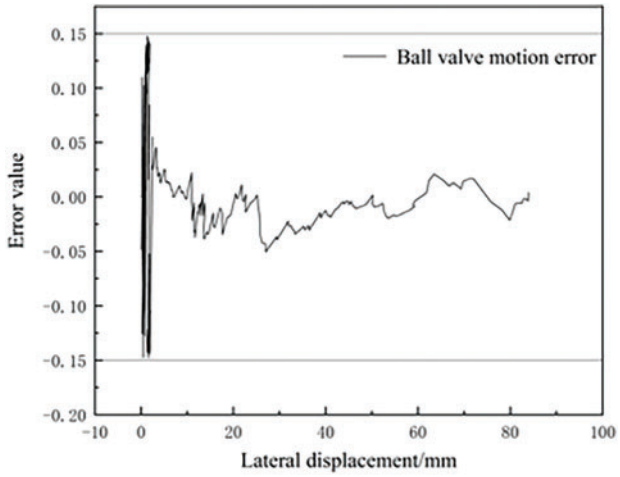

Figure 28: Ball valve motion error curve

5 Conclusion

Taking the Y Check (automatic steering tool) from RMS Company as the research object, a combined experimental and numerical simulation method was employed to study the opening and closing performance of the steering tool. A solution method suitable for bidirectional fluid-structure coupling problems, considering spring stress accumulation, was proposed. The opening and closing performance simulation analysis of the steering tool was completed and experimentally verified, leading to the following main conclusions:

1. With the sector spring thickness of 1.2 mm and width of 40 mm, a solution method for bidirectional fluid-structure coupling problems, considering spring stress accumulation, was proposed. Using the prestress field in ABAQUS software to define the stress changes in the sector spring and the ball valve as a medium, the transmission of flow field forces and the motion of the ball valve were analyzed with FLUENT software. This allowed for the generation of the performance parameter curve of the steering tool. The results showed that under the designed conditions, the response time for the ball valve to switch from steam injection to oil extraction was approximately 0.0787 s. The motion path closely conformed to the designed trajectory, the motion remained relatively stable, and the opening and closing performance of the steering tool was found to be satisfactory.

2. An indoor experimental rig was designed and constructed, and an indoor test experiment of the steering tool was carried out using a high-speed camera. The motion time and path of the ball valve in the simulation and experiment were largely consistent, with a motion time error of approximately −11.5%, and the maximum error in the ball valve motion path did not exceed 15%. This validated the accuracy of the numerical simulation results and provided theoretical support for the practical application of the steering tool.

Although effective numerical analysis and experimental validation of the opening and closing performance of the steering tool have been provided, several research gaps remain, including: exploring the performance of the steering tool under different operational conditions (e.g., varying fluid temperatures and pressures) and optimizing the design to improve its stability and response time; further refining the fluid-structure coupling model, considering additional nonlinear factors, to better predict the long-term performance of the steering tool, especially with respect to the accumulation of spring stress. These efforts would provide stronger theoretical support and technical assurance for the practical application of integrated injection-production tubing string technology.

Acknowledgement: The authors thank all the editors and anonymous reviewers for their comments and suggestions.

Funding Statement: The authors received no specific funding for this study.

Author Contributions: Xianjun Zhou, Yuxuan Peng: Conceptualization, Methodology, Writing—Original Draft. Wenjia Cheng, Yangfan Xue: Data Curation, Formal Analysis. Hao Fang: Review & Editing. All authors reviewed the results and approved the final version of the manuscript.

Availability of Data and Materials: The datasets generated and/or analyzed during this study are not publicly available due to privacy restrictions for the paper's authors. Reasonable requests for data access should be directed to the corresponding author.

Ethics Approval: Not applicable.

Conflicts of Interest: The authors declare no conflicts of interest to report regarding the present study.

References

1. Zou CN, Zhai GM, Zhang GY, Wang HJ, Zhang GS, Li JZ, et al. Global conventional-unconventional oil and gas formation, distribution, resource potential and trend prediction. Pet Explor Dev. 2015;42:13–25.
2. Xiao S, Zhao S, Yang H. Advances in unconventional oil and gas geological theory and exploration technology. Shandong Chem Ind. 2021;50(7):65–6. doi:10.19319/j.cnki.issn.1008-021x.2021.07.024.
3. Xue L, Shi Z, Ma L, Zhao Y, Yue S, Hong L, et al. Hydrocarbon accumulation models and exploration potential of MesoCenozoic heavy oil in northern Melut Basin, South Sudan. Lithol Reserv. 2023;35(3):76–85. doi:10.12108/yxyqc.20230307.
4. Xing H, Zhang J, Zhang Q, Zhang Y, Zhang C, Ma X. Single well production-injection integration technology for the EP18-1 Oilfield in South China Sea. Offshore Oil. 2019;39(4):23–7. doi:10.3969/j.issn.1008-2336.2019.04.023.
5. Cui Z, Zhang J, Cai H, Zhang C. Field test of multifaceted thermal fluid throughput technology in Bohai oilfield. J Chang Univ Auton Sci Ed. 2014;11(32):115–8. doi:10.16772/j.cnki.1673-1409.2014.32.035.
6. Xiao L, Zhang G. The strength analysis of contact leaf spring by ANSYS. Mod Manuf Eng. 2011;1:119–22. doi:10.16731/j.cnki.1671-3133.2011.01.013.

7. Hu X. Numerical algorithms for a class of fluid-structure coupled problems and physical simulation of swaying trees in a wind field [dissertation]. Hangzhou, China: Zhejiang University; 2008.
8. Wang Z, Liu Z, Xu N. Modeling and dynamic characteristic investigation of elastic ring squeeze film damper by fluid-structure interaction approach. Turbine Technol. 2020;62(1):1–5.
9. Li M, Zhao PF, Wang GH, Liu J. Numerical analysis on high speed liquid-solid impact of 17-4PH material. Appl Mech Mater. 2014;548-549:147–51. doi:10.4028/www.scientific.net/AMM.548-549.147.
10. Yao Y, Zheng X, Ma QW, Zhou ZL. Study on dynamic characters of side-by-side elastic plate using two-way fluid-structure coupling method. In: The 32nd International Ocean and Polar Engineering Conference; 2022 Jun 5–10; Shanghai, China.
11. El Hadi Attia M, Zayed ME, Kabeel AE, Khelifa A, Arıcı M, Abdelgaied M. Design and performance optimization of a novel zigzag channeled solar photovoltaic thermal system: numerical investigation and parametric analysis. J Clean Prod. 2024;434:140220. doi:10.1016/j.jclepro.2023.140220.
12. Attia ME, Zayed ME, Kabeel AE, Khelifa A, Irshad K, Rehman S. Numerical analysis and design of a novel solar photovoltaic thermal system using finned cooling channel structures embedded with air/TiO_2–water nano bi-fluid. Sol Energy. 2024;269:112368. doi:10.1016/j.solener.2024.112368.
13. Liang Z. Characterization of hydrodynamic vibration of 90-degree elbow based on bidirectional fluid-solid coupling [master's thesis]. Daqing, China: Northeast Petroleum University; 2021. doi:10.26995/d.cnki.gdqsc.2021.000496.
14. Bradley HB. Handbook of petroleum engineering. Beijing, China: Petroleum Industry Press; 1992. p. 200–300.
15. Li P, Xu M, Wang F. Mastering CFD engineering simulation and case practice: FLUENT GAMBIT ICEM CFD Tecplot [Online]. Beijing, China: Posts & Telecom Press; 2011 [cited 2025 Jan 1]. Available from: https://book.douban.com/subject/6865594/.
16. Wang Z, Shen X. Fundamentals of tribological design. Beijing, China: Beijing University of Aeronautics and Astronautics Press; 2018. p. 220–40.
17. Yang N, Wu X, Liang S, Qin M, Zhu F, Wang H, et al. Research on stiffness characteristics of hold-down spring based on Johnson-Cook constitutive model. Nucl Power Eng. 2022;43(4):91–8. doi:10.13832/j.jnpe.2022.04.0091.
18. Zhou XJ, Li H, Peng Y, Yu F, Fang H. Research on the characteristics of shaped leaf springs in integrated injection-production automatic steering tools. Mod Manuf Eng. 2025;1:71–79, 120. doi:10.16731/j.cnki.1671-3133.2025.01.009.